Cellular Physiology and Biochemistry

Cell Physiol Biochem 2018;50:1186-1200
DOI: 10.1159/000494546
Published online: 24 October 2018
Accepted: 16 October 2018

Original Paper

Glt25d2 Knockout Directly Increases $CD25^+CD69^-$ but Decreases $CD25^-CD69^+$ Subset Proliferation and is Involved in Concanavalin-Induced Hepatitis

Xiaohua Hao[a] Ran Liu[a] Yifan Zhang[a] Yufeng Li[a] Qun He[b]
Yubo Huang[a] Yu Jiang[c] Jiali Ma[c] Ping Li[c] Hongshan Wei[c]

[a]Institute of Infectious Disease, Beijing Ditan Hospital, Capital Medical Univerisity, Beijing, [b]Biochip Center, the key laboratory of cell biology, Ministry of Education, College of Basic Medicine Science, China Medical University, Shenyang, [c]Department of Gastroenterology, Beijing Ditan Hospital, Capital Medical Univerisity, Beijing, China

Key Words
$CD4^+$ T lymphocyte • Glycosylation • Proliferation • GLT25D2 • Gene knockout

Abstract
Background/Aims: The elaborate structure of the extracellular matrix (ECM) and the appropriate surface glycoforms upon it are indispensable to $CD4^+$ T cell regulation. ***Methods:*** To explore the effects of Glcα1,2Galβ1 glycosylation mediated by GLT25D2 (Colgalt2) for $CD4^+$ T cell regulation, we prepared C57BL/6J *Glt25d2*$^{-/-}$ mice. In the induction of hepatitis, after concanavalin A (Con A) challenge for 6, 12, and 24 h, more extensive parenchymal injury was noted in *Glt25d2*$^{-/-}$ mice than in wild-type (WT) mice at 12 h. Immunohistochemistry and laser scanning confocal microscopy were used to detect GLT25D2 expression, and subsets of CD4+T cells was analyzed by flow cytometry. A total of 26 cytokines in serum samples were determined using Luminex technology. ***Results:*** The trend in liver injury score variation was consistent with serum alanine aminotransferase and aspartate aminotransferase levels. The levels of interleukin 4 (IL-4), IL-1β, IL-9, and several chemokines such as macrophage inflammatory protein-2, eotaxin, and growth-related oncogene α were significantly increased in *Glt25d2*$^{-/-}$ mice compared with WT mice after Con A challenge. A further phenotype analysis of primary *Glt25d2*$^{-/-}$ $CD4^+$ T cells showed that *Glt25d2* knockout increased the frequency of the $CD25^+CD69^-$ subset but decreased the frequency of the $CD25^-CD69^+$ subset after Con A challenge for 6, 12, and 24 h compared with those of WT $CD4^+$ T cells. Activation-induced apoptosis was also significantly increased in *Glt25d2*$^{-/-}$ $CD4^+$ T cells after Con A challenge compared with WT $CD4^+$ T cells. Lectin microarray hybridization showed that *Glt25d2* knockout increased the binding activity of *Narcissus pseudonarcissus* lectin to $CD4^+$ T cells but

X. Hao and R. Liu contributed equally to this work.

Prof. Hongshan Wei
Department of Gastroenterology, Beijing Ditan Hospital, Capital Medical Univerisity
No.8, Jinshun Eaststreet, Chaoyang District, 100015, Beijing (China)
E-Mail drwei@ccmu.edu.cn

Amaranthus caudatus lectin–binding activity was lost during Con A challenge. ***Conclusion:*** The present results suggest that collagen glycosylation mediated by GLT25D2 may regulate a subset of $CD4^+$ T cells and be involved in the pathogenesis of Con A–induced hepatitis.

Introduction

Over the past half century, extracellular matrix (ECM) research has shown that matrix components play a fundamental role in immunity, including in immune cell development, effector regulation, and ligand–receptor interactions [1-3]. The function of T lymphocytes involved in an immune response is dependent on the precise matrix structure of the ECM. The dynamic variation of the ECM is indispensable for the migration and activation of effector T cells. Some ECM components, such as proteoglycans, can also act as signaling molecules, endogenous ligands of Toll-like receptors, activators of the innate immune response, and mediate activators of the adaptive immune response during inflammation [4, 5]. The ECM can also modify major histocompatibility complex class II expression in the pathological state [6].

Collagen proteins are the most abundant components in the ECM, constituting >30% of the total protein mass in multicellular organisms. Therefore, genetic defects of collagen formation affect almost every organ system and tissue throughout the body [7]. Among the genomes of vertebrates and higher invertebrates, 28 distinct collagen glycoproteins are encoded by at least 45 genes [8]. The primary structure of a collagen protein consists of Gly-Xaa-Yaa repeats and forms a left-handed polyproline II–like helix. Three glycopeptide chains align with an offset right-handed superhelix. Each peptide chain has at least one collagenous and one non-collagenous domain, variations of which depend on the specific collagen type [9].

After initiating translation, the pro-collagen peptide translocating into the endoplasmic reticulum (ER) is co-translationally modified by hydroxylation and glycosylation of lysine and hydroxylysine, respectively. Mature collagen molecules are modified by Glcα1, 2Galβ1-glycan on the hydroxylysine residue. The glycosylated levels of collagen proteins vary among tissues and organs. Since the first report nearly 60 years ago showed that collagen contains a galactose or glucosylgalactose O-glycosidically linked to the hydroxylysine residue, it was of interest to explore which glycosyltransferase plays a critical role in this glycosylation process [10, 11]. At the start of this century, lysyl hydroxylase 3 (EC 1.14.11.4) was found to possess the activities of galactosyltransferase (EC 2.4.1.50) and glucosyltransferase (EC 2.4.1.66) [12]. Schegg and colleagues recently reported that human collagen glycosylation is initiated by two β(1-O)galactosyltransferases *in vitro*, specifically GLT25D1 (Colgalt1) and GLT25D2 (Colgalt2) [13].

In the ECM, the elaborate collagen structure is critical for coordinating lymphocyte homing, differentiation, and activation, as well as targeting migration [14, 15]. More importantly, some glycan components in the ECM may enhance T cell activation and trigger autoimmune inflammation [16]. Some collagen molecules, such as elastin peptides, can directly regulate immune responses in aging and age-related diseases [17]. In fact, peripheral $CD8^+$ T cell activation was directly triggered by the ECM, as seen for those cells from mesenteric lymph nodes *in vivo* [18]. These results suggested that the glycan structure of collagen plays an important role in T lymphocyte regulation, but as far as we have seen, no relevant data are available. Consequently, the elucidation of the interaction between collagen glycosylation and lymphocyte regulation is essential for generating effective immunotherapies.

Many components of the ECM are correlated with $CD4^+$ T lymphocyte regulation, such as laminins [19], proteoglycan aggrecans [20], and integrin [21, 22]. The co-culturing of $CD4^+$ T cells with fibroblasts significantly increased the secretion of IL-17 and other cytokines [23]. These results suggested that the ECM and its elaborate construction is indispensable to the functional regulation of $CD4^+$ T lymphocytes. As a major component of the ECM, its extent and pattern of glycosylation directly regulate cross-link maturation in fibrillar collagen [24,

25]. More importantly, almost all ECM components are glycoproteins since these components require trafficking from a secretory pathway (from the ER to the Golgi complex) to the ECM. $CD4^+$ T regulation may be dependent on collagen glycosylation to some degree. As far as we have seen, there is currently no evidence available to answer this question.

To address this question, we recently prepared a *Glt25d2*-knockout (*Glt25d2*$^{-/-}$) mouse model [26]. The intravenous injection of concanavalin A (Con A) is a widely used model for acute immune-mediated hepatitis in mice [27]. Since $CD4^+$ T lymphocytes as well as NKT cells are the major effector cells involved in Con A hepatitis [28], the Con A–induced hepatitis model was chosen to elucidate the role of $CD4^+$ T cells in *Glt25d2*$^{-/-}$ mice. CD25 and CD69 are activation markers of T lymphocytes [29]. The emergence of CD25 molecules can occur if $CD4^+$ T cells are activated and proliferating [30]. As the best-characterized populations of regulatory T cells, $CD4^+CD25^+$ T cells have important roles in maintaining normal homeostasis and play a crucial role in infectious and degenerative diseases [31].

Our present results suggest that *Glt25d2* knockout regulates the subset frequency of $CD4^+$ T cells and is involved in the pathogenesis of Con A–induced hepatitis.

Materials and Methods

Preparation of Glt25d2$^{-/-}$ *mice and ethics statement*

To elucidate the role of GLT25D2 in liver injury, we recently prepared *Glt25d2*$^{-/-}$ mice using a gene-targeting method [26]. The sense primer (loxp-F) 5′-ATGTCCTGTCTAGTGTGGTCC-3′ and antisense primer (Loxp-R) 5′- agggagttgtgcgaatctat-3′ were used to genotype the wild-type (WT) and *Glt25d2*$^{-/-}$ mice. Western blotting was used to further confirm *Glt25d2* knockout (polyclonal anti-GLT25D2; Abcam, Cambridge, UK).

The experimental mice were raised in the Animal Center of Peking University Health Science Center according to the National Institutes of Health Guide for the Care and Use of Laboratory Animals. This study was approved by the Experimental Animal Care and Use Committee of Peking University Health Science Center.

Animals and hepatitis model

To create the Con A–induced hepatitis model, male mice (6–8 weeks old) were used in this experiment [27]. Specific-pathogen-free WT (*Glt25d2*$^{+/+}$) C57BL/6J mice (Animal Center of Peking University Health Science Center, Beijing, China) were used as control animals. Each was maintained in a specific-pathogen-free condition at the Animal Center of Peking University Health Science Center. All experimental mice were housed under standard conditions (22–24°C) with a light-dark cycle of 12:12 h. Sterile water and food were available *ad libitum*. The hepatitis model was induced by an intravenous injection of 10 mg/kg Con A (Sigma-Aldrich, St. Louis, MO) and the liver injury was assessed before and 6, 12, and 24 h after Con A administration. The liver injury was assessed as serum levels of alanine aminotransferase (ALT) and aspartate aminotransferase (AST). The injury score was used to evaluate the hepatic tissue staging as previously reported [32]. The study design is shown in Fig. 1.

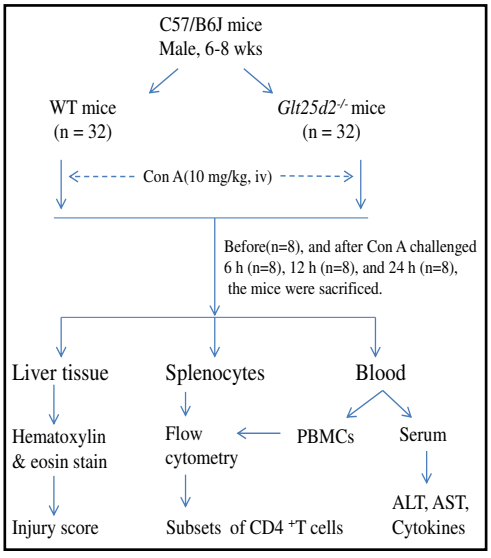

Fig. 1. Study design (*in vivo*).

Immunohistochemistry and laser scanning confocal microscopy

After the mice were sacrificed, the liver and spleen tissues were obtained at different time points after Con A injection. The tissues were fixed with 10% formaldehyde, embedded in paraffin, and cut into 3- to 5-μm sections. Hematoxylin and eosin (H&E) staining was used to evaluate liver injury grade. After

antigen retrieval was completed in sodium citrate buffer (pH 6.0 for 10 min), the endogenous peroxidase was blocked for 5 min. Sections were incubated for 1 h at room temperature with anti-GLT25D2 antibody (1:500). After incubation with the secondary horseradish peroxidase–conjugated immunoglobulin G, DAB chromogen was used to detect GLT25D2 expression in the hepatic and splenic tissues.

We subcloned the coding sequence of *Glt25d2* into the pDSRED-N1 plasmid. The pDSRED-Glt25d2-N1 plasmid was then transfected into HSC-T6 cells to express GLT25D2 recombinant protein with red fluorescence. The coding sequence of the ER–Golgi intermediate compartment 53 (ERGIC53) protein [33, 34] was subcloned into the pEGFP-C1 plasmid to construct the pEGFP-ERgic53-C1 plasmid, which expresses recombinant ERGIC53 protein with green fluorescence. DAPI staining was performed 48 h after co-transfection of the pDSRED-Glt25d2-N1 and pEGFP-ERgic53-C1 plasmids into HSC-T6 cells. Confocal laser scanning microscopy (Zeiss LSM 510, Oberkochen, Germany) was used to analyze the GLT25D2 and ERGIC53 expression in the HSC-T6 cells.

Flow cytometry analysis of CD4⁺ subsets in peripheral blood mononuclear cells and splenocytes

To detect surface markers of $CD4^+$ T cells, peripheral blood mononuclear cells and splenocytes were stained with CD4-APC, CD8-perCP, CD25-PE, and CD69-FITC antibodies (eBioscience, San Diego, CA) and incubated for 20 min at 4°C in the dark. After washing, we performed flow cytometry analysis (FACSCalibur flow cytometer; BD Biosciences, San Jose, CA) of the $CD4^+$ T cell subsets. At least 10, 000 live events were accumulated through forward- and side-scatter parameters. CellQuest Pro software (BD Biosciences) was used to analyze the flow cytometry data.

Primary CD4⁺ T cell proliferation and apoptosis in vitro

Splenocytes were harvested from the WT and *Glt25d2*$^{-/-}$ mice by dissociation through a 0.45-μm wire mesh. After lysing erythrocytes using ammonium chloride, the cells were subsequently resuspended in complete RPMI 1640 media containing 10% fetal calf serum, L-glutamine, penicillin, and streptomycin. To isolate the $CD4^+$ T cells, the magnetic bead sorting technique (EasySep Mouse $CD4^+$ T Cell Isolation Kit; Miltenyi Biotec, Bergisch Gladbach, Germany) was used. Briefly, splenocytes were incubated with anti-CD4 microbeads for 15 min at 4°C following the manufacturer's instructions. After washing with PBEB buffer (phosphate buffered saline [PBS], 0.5% bovine serum albumin, 5 mM ethylenediaminetetraacetic acid), the $CD4^+$ T cells were eluted from the LS columns and resuspended in RPMI 1640 media. After culturing in RPMI 1640 media for 12 h, the $CD4^+$ T cells were treated with Con A (5 μg/mL) for another 6, 12, or 24 h. For the subset analysis, $CD4^+$ T cells from the WT and *Glt25d2*$^{-/-}$ mice were incubated with fluorescently tagged antibodies against CD4, CD8, CD25, and CD69 (eBioscience) for 30 min at room temperature in the dark. Before the analysis, the stained $CD4^+$ T cells were washed with cold PBS.

For the apoptosis evaluation, the $CD4^+$ T cells from the WT and *Glt25d2*$^{-/-}$ mice were incubated in medium containing Con A for 0, 6, 12, or 24 h. The cells were labeled with an apoptosis marker (Annexin V, 7-AAD) for the subset analysis. Briefly, after being labeled with CD4 antibody, the cells were washed with PBS and resuspended in binding buffer. After anti-Annexin V fluorescently tagged antibody and 7-AAD were added, the $CD4^+$ T cells were incubated for 10 min in the dark at 37°C. Apoptosis was calculated as the percentage of 7-AAD^+ and Annexin V^+ cells.

Cytokine determination

A total of 26 cytokines in serum samples were determined using Luminex technology with Milliplex detection kits (Millipore, Burlington, MA) according to the manufacturer's protocols. Those cytokines included interleukins and nine chemokines.

Table 1. Lectin spot microarray used in this study

Lectin location No. on array	Lectin names	abbreviation
1	Lotus tetragonolobus lectin	LTL
2	Pisum sativum agglutinin	PSA
3	Lens culinaris agglutinin	LCA
4	Ulex europaeus lectin type 1,	UEA-1
5	Aurentia lectin	AAL
6	Maackia amurensis lectin I	MAL-I
7	Maackia amurensis lectin II	MAL-II
8	Sambucus nigra	SNA
9	Wheat germ agglutinin	WGA
10	Erythrina cristagalli lectin	ECL
11	Datura stramonium agglutinin	DSA
12	Solanum tuberosum lectin	STL
13	Succinylated WGA	SWGA
14	Helix pomatia agglutinin	HPA
15	Canavalia ensiformis	ConA
16	Galanthus nivalis agglutinin	GNA
17	Hippeastrum hybrid lectin	HHL
18	Bauhinia purpurea lectin	BPL
19	Euonymus europaeus lectin	EEL
20	Jackfruit lectin	Jacalin
21	Wisteria floribunda lectin	WFA
22	Amaranthus caudatus lectin,	ACL
23	Maclura pomifera lectin	MPL
24	Dolichos biflorus agglutinin	DBA
25	Soybean agglutinin	SBA
26	Narcissus pseudonarcissus leptin	NPL

Lectin microarray and hybridization

The lectin microarray was prepared as previously described [35, 36]. Briefly, lectins (Vector Laboratories, Inc., Burlingame, CA) (Table 1) were dissolved in spotting solution at a concentration of 1 mg/mL (*Sambucus nigra* leptin, MAL-I, and MAL-II) or 0.5 mg/mL (other lectins) and spotted in duplicate onto a 3-glycidoxypropyltrimethoxysilane glass slide using a microarray printing robot (MicroGridII; BioRobotics Ltd., Cambridge, UK). After being spotted, washed, and incubated, the slides were blocked with 1% bovine serum albumin. Purified $CD4^+$ T cells from the spleens of WT and *Glt25d2*$^{-/-}$ mice were cultured in RPMI 1640 media. Before and after Con A treatment for 6, 12, or 24 h, the harvested $CD4^+$ T cells were suspended in PBS and allowed to bind to lectin microarrays at 37°C for 30 min. The unbound $CD4^+$ T cells were washed with cold PBS. The bound $CD4^+$ T cells immobilized on the glass slides were stained with H&E and observed by microscopy.

Statistical analysis

The quantitative results are represented as the mean ± SEM. Intergroup differences were tested using Student's *t* test or the Mann-Whitney *U* test. Differences among multiple groups were analyzed using one-way analysis of variance. Statistical significance was defined as values of $P < 0.05$. These analyses were performed using GraphPad Prism version 5.01 software.

Results

GLT25D2 expressed in hepatic and splenic tissues

Using our previously prepared *Glt25d2*$^{-/-}$ mice, we first confirmed the genotype and phenotype using polymerase chain reaction (Fig. 2A) and western blotting (Fig. 2B), respectively. We further evaluated GLT25D2 expression in the hepatic and splenic tissues of WT and *Glt25d2*$^{-/-}$ mice by immunohistochemical (IHC) staining. As we speculated, there was no GLT25D2 protein expression in the tissues of the *Glt25d2*$^{-/-}$ mice; however, IHC staining revealed that the GLT25D2 protein was expressed in the hepatic and splenic tissues of WT mice (Fig. 2C–E).

GLT25D2 expressed in hepatic and splenic tissues

The C-terminus of GLT25D2 contains the RDEL motif, an ER retrieval signal, suggesting that it is a resident protein in the ER according to a recent report [36]. The confocal laser scanning microscopy images show that GLT25D2 protein and ERGIC53 protein were colocalized in the ER (Fig. 2F).

Glt25d2 knockout aggravates liver injury

We first determined whether GLT25D2 was involved in Con A–induced liver injury. Con A (10 mg/kg) was injected into healthy WT mice and *Glt25d2*$^{-/-}$ mice to prepare the Con A–induced hepatitis model. H&E staining showed that Con A administration resulted in more extensive hepatocellular damage in *Glt25d2*$^{-/-}$ mice than in WT mice, as represented by the presence of a severely collapsing liver plate (Fig. 3). The liver injury scores of *Glt25d2*$^{-/-}$ mice were increased after Con A challenge for 12 h (3.5 ± 0.45; $P = 0.02$) compared with those of *Glt25d2*$^{-/-}$ mice after 12 h (2.88 ± 0.44). However, there was no difference in injury scores between *Glt25d2*$^{-/-}$ and WT mice after Con A challenge for 6 or 24 h (1.71 ± 0.49, $P = 0.32$; 3.58 ± 0.49 *vs* 3.50 ± 0.44, $P = 0.71$, respectively). This variation trend was consistent with the serum ALT and AST levels. Although those mice were raised in the same conditions, the ALT levels (58.83 ± 15.28 U/L) of the *Glt25d2*$^{-/-}$ mice were significantly higher than those of the WT mice (43.38 ± 10.54 U/L, $P = 0.04$) at baseline. After Con A administration for 6 h (6738.0 ± 3524.0 U/L *vs* 2101 ± 1811 U/L, $P = 0.01$) or 12 h (15060.0 ± 8052.0 U/L *vs* 7041.0 ± 2056 U/L, $P = 0.02$), this difference was more significant (Fig. 3). The same variation trend was also observed in serum AST levels before and after Con A challenge between WT and *Glt25d2*$^{-/-}$ mice (Fig. 3).

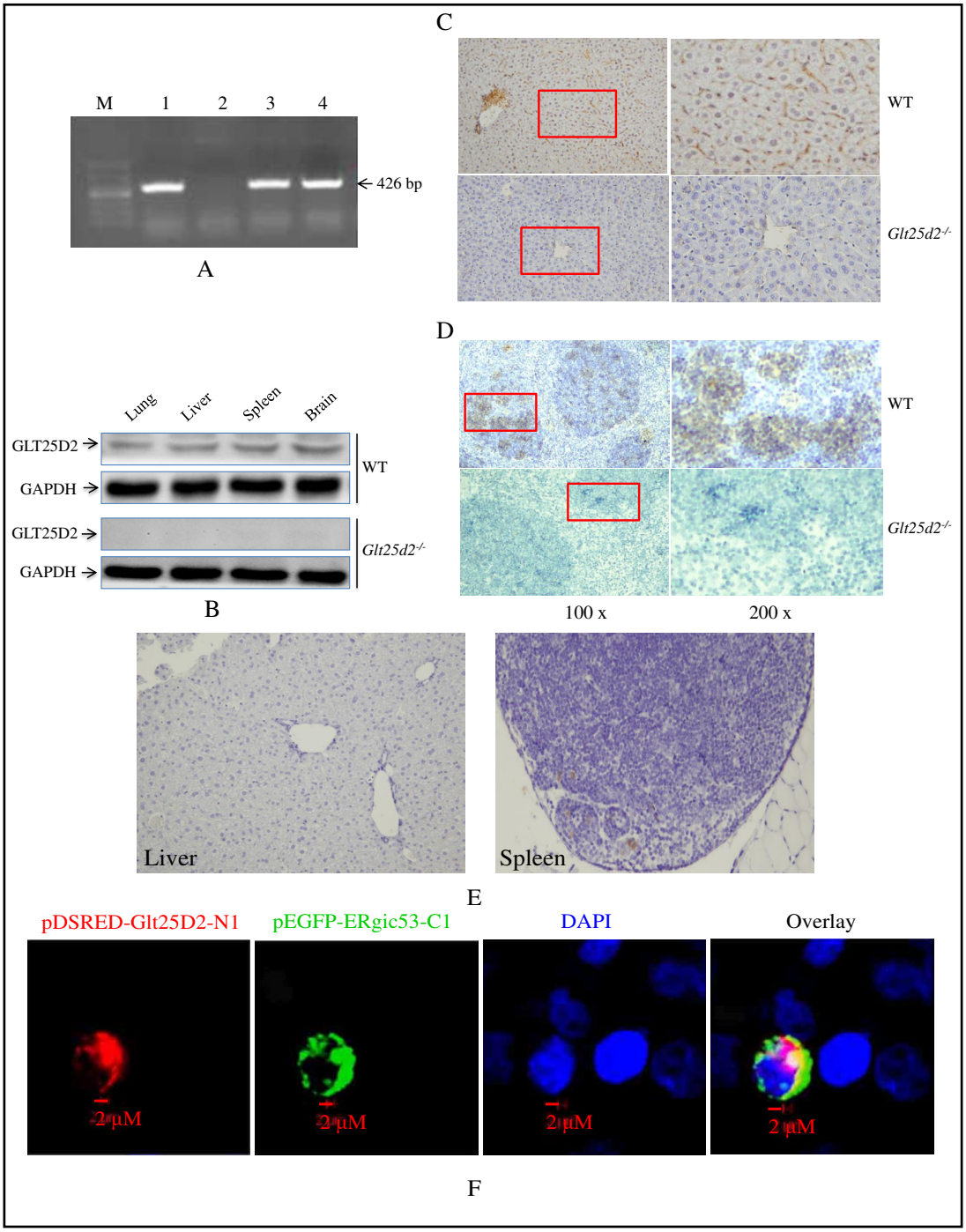

Fig. 2. Immunohistochemical staining of GLT25D2 expression in hepatic and splenic tissues. A, GLT25D2 protein in the hepatic tissue of wild-type mice was mainly expressed in the interstitial region. B, Major expression was seen in the germinal center of splenic tissue, whereas no expression was seen in the hepatic and splenic tissues of Glt25d2$^{-/-}$ mice. C, GLT25D2 protein was expressed in the hepatic tissues of WT mice. D, GLT25D2 protein was expressed in the splenic tissues of WT mice. E, Isotype control liver and spleen tissue. F, Confocal laser scanning microscopy images show that GLT25D2 and ERGIC53 proteins were co-localized in the endoplasmic reticulum.

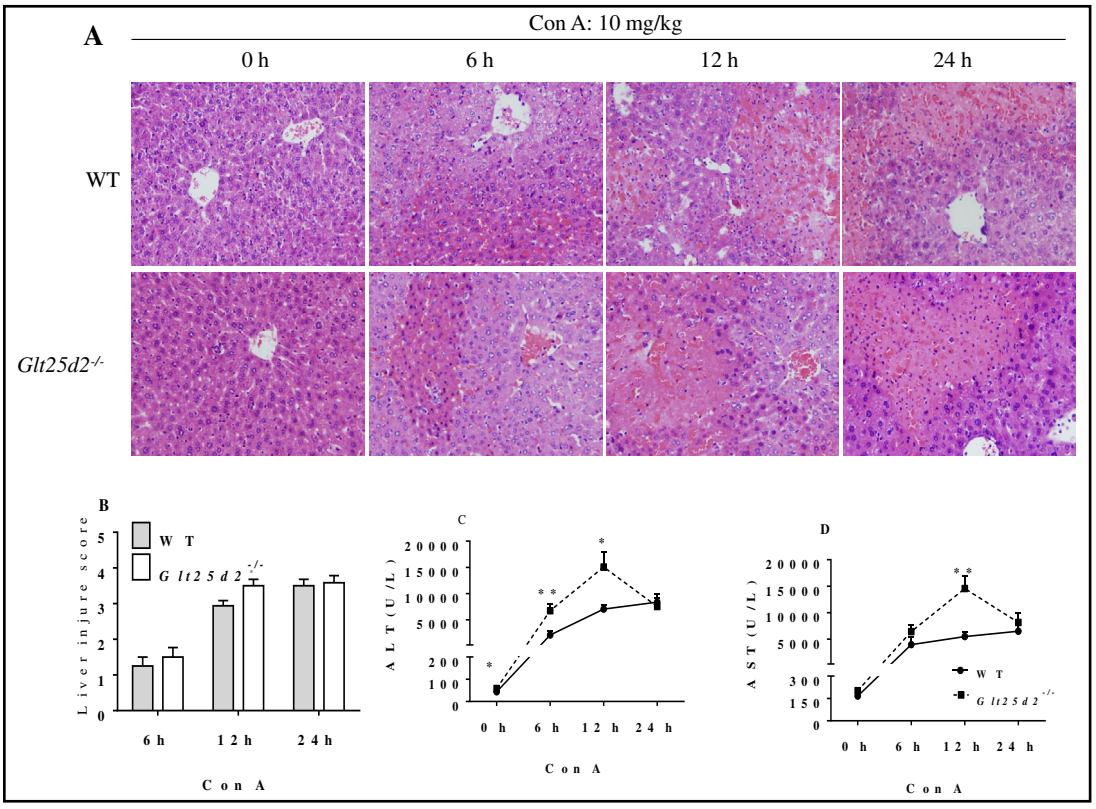

Fig. 3. Liver injury score and serum biochemical analysis. A, Hematoxylin and eosin staining of hepatic tissue (×200). After concanavalin A (Con A) administration for 6, 12, or 24 h, centrilobular hemorrhagic necrosis was seen in the hepatic tissue. The injury score for lobular inflammation was as reported previously [50]. B, Compared with tissues of wild-type mice, more intensive necrosis was visible in the Glt25d2$^{-/-}$ mouse hepatic tissue after Con A challenge for 12 h. C, D, Alanine aminotransferase and aspartate transferase levels varied before and after Con A challenge for 0, 6, 12, or 24 h (*P<0.05; **P<0.01).

Different cytokine profiles between WT and Glt25d2$^{-/-}$ mice

To characterize the inflammatory response more completely between WT and *Glt25d2*$^{-/-}$ mice, we performed Luminex analysis of the serum. After Con A challenge for 6 h (25.79 ± 4.32 pg/mL) or 12 h (18.43 ± 4.41 pg/mL), the serum IL-1β levels of the *Glt25d2*$^{-/-}$ mice were markedly increased compared with those of the WT mice (17.5 ± 3.9 pg/mL, $P = 0.002$; and 10.43 ± 2.79 pg/mL, $P = 0.003$). After Con A challenge for 6, 12, or 24 h, the levels of IL-4, IL-6, and IL-9 were also significantly increased in *Glt25d2*$^{-/-}$ mice compared with those in WT mice (Fig. 4). This trend was also observed with some chemokines, including macrophage inflammatory protein 2 (MIP-2), eotaxin, and growth-related oncogene α (GROα) (Fig. 4). The notable result is the serum IL-9 level. After Con A administration for 6, 12, and 24 h, the serum IL-9 level was decreased in WT mice but significantly increased in *Glt25d2*$^{-/-}$ mice after Con A challenge for 12 h (19.09 ± 11.54 pg/mL *vs* 7.82 ± 5.26 pg/mL, $P = 0.02$). No differences in serum levels of other cytokines were observed between WT and *Glt25d2*$^{-/-}$ mice, such as IL-17, IL-23, IL-27, IL 12p70, MCP-3, MIP-1a, MIP-1b, and RANTES (data not shown).

Phenotype analysis of blood and splenic subsets of CD4$^+$ T cells

To investigate whether proliferation in CD4$^+$ T cell subsets plays a role in Con A–induced liver injury, we studied the characteristics of CD4$^+$ T cell subsets of Con A–challenged mice. Con A administration induced a significant decrease in the frequency of the CD25$^+$CD69$^+$ subset in the blood of *Glt25d2*$^{-/-}$ mice (17.85% ± 5.52% *vs* 33.24% ± 3.96%, $P < 0.0001$) 12

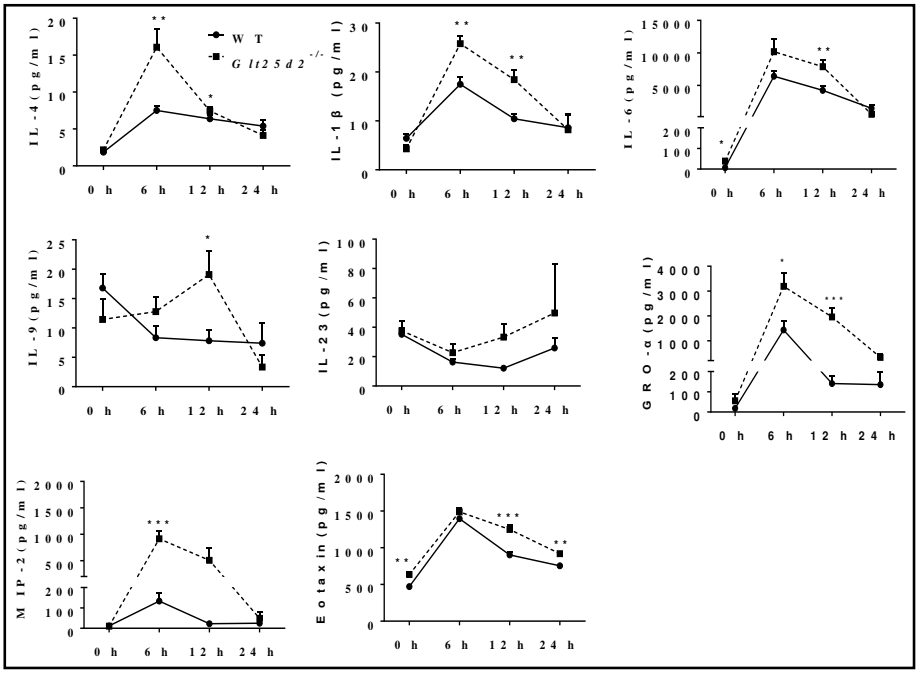

Fig. 4. Serum cytokines before and after concanavalin A challenge. Luminex technology was used to determine the serum levels of 26 cytokines (*P < 0.05; **P < 0.01; ***P<0.001).

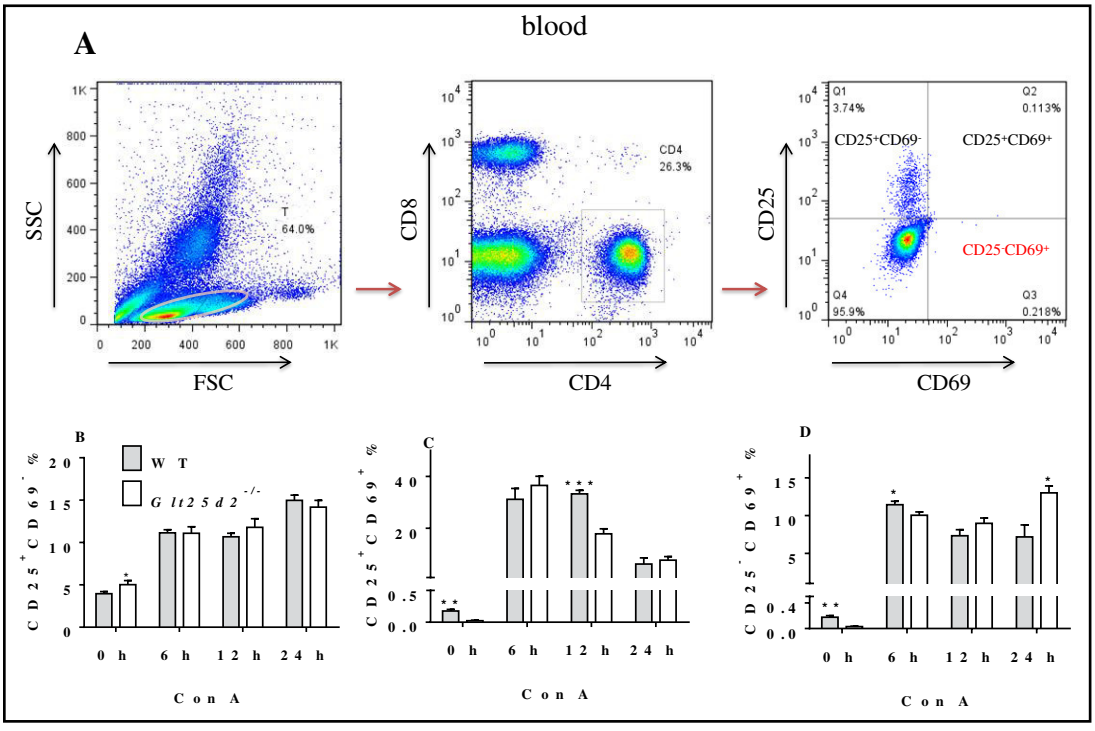

Fig. 5. Phenotype analysis of blood subsets of CD4+ T cells. A, Gating method used to identify CD4+T cells and their subsets. B–D, The column diagram shows $CD25^+CD69^-$ (B), $CD25^+CD69^+$ (C), and $CD25^-CD69^+$ (D) subsets of $CD4^+$ T cells in the blood before and after concanavalin A challenge for 0, 6, 12, or 24 h.

h after challenge, but the frequency of the $CD25^-CD69^+$ subset was markedly increased at 24 h (13.02% ± 2.06% *vs* 7.17% ± 3.55%, $P = 0.01$) compared with those of WT mice (Fig. 5). Interestingly, the increased frequency of the $CD25^+CD69^-$ subset was only seen in the spleens of *Glt25d2*$^{-/-}$ mice after Con A challenge for 12 h (13.52% ± 2.88% *vs* 9.97% ± 1.38%, $P = 0.007$) and 24 h (15.90% ± 3.26% *vs* 7.60% ± 2.94%, $P = 0.0009$); the frequency of the

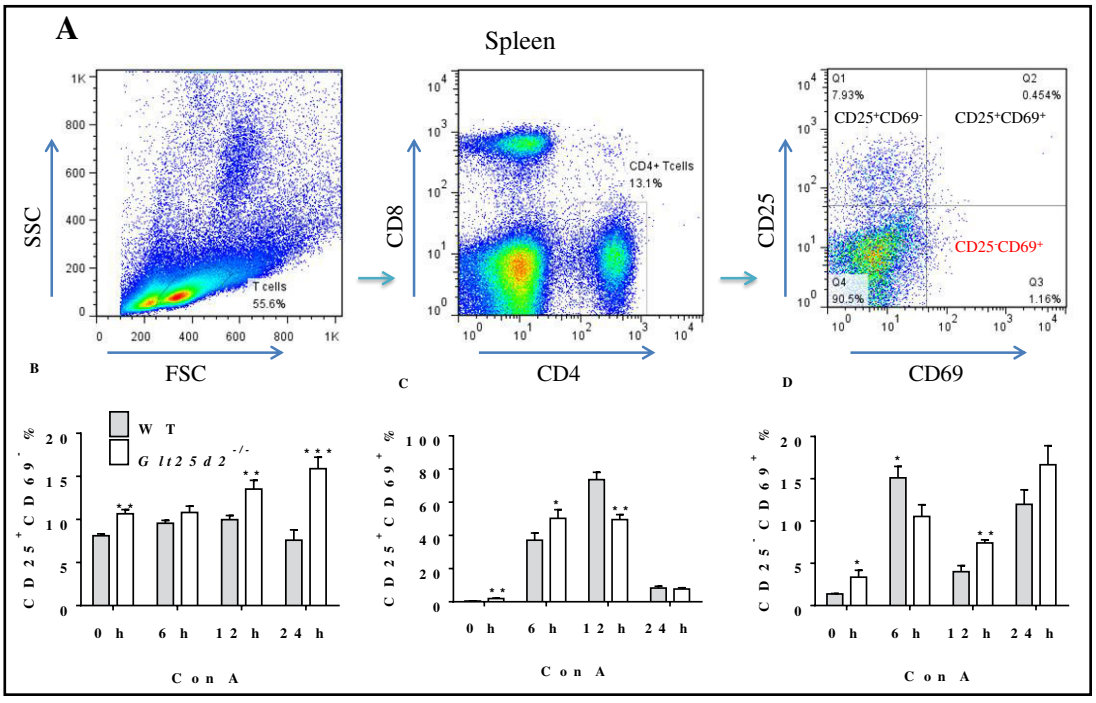

Fig. 6. Phenotype analysis of spleen subsets of CD4+ T cells. A, Gating method used to identify CD4+T cells and their subsets. B–D, The column diagram shows $CD25^+CD69^-$ (B), $CD25^+CD69^+$ (C), and $CD25^-CD69^+$ (D) subsets of CD4+ T cells in the spleen before versus after concanavalin A challenge for 0, 6, 12, or 24 h (*P<0.05; **P<0.001; ***P<0.0001).

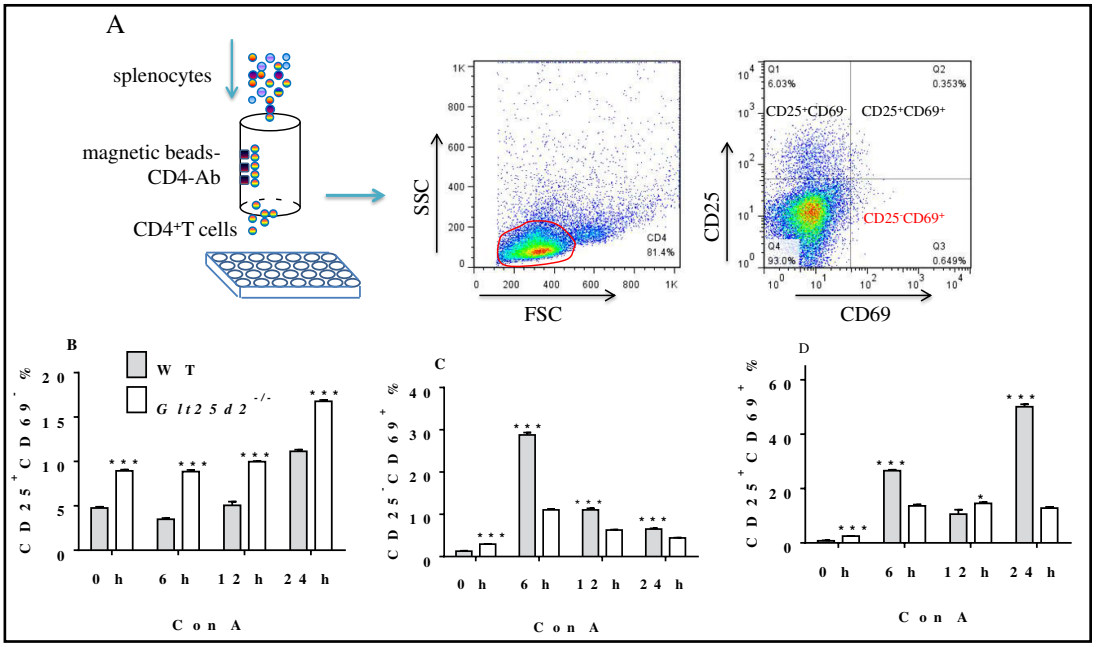

Fig. 7. Phenotype analysis of primary CD4+ T cells isolated from splenocytes (ex vivo). A, Primary CD4+ T cells isolated from splenocytes were analyzed before and after concanavalin A (Con A) challenge for 0, 6, 12, or 24 h. B–D, The column diagram shows $CD25^+CD69^-$ (B), $CD25^+CD69^+$ (C), and $CD25^-CD69^+$ (D) subsets of CD4+ T cells in the spleen before versus after Con A challenge for 0, 6, 12, or 24 h (*P<0.05; **P<0.001; ***P<0.0001).

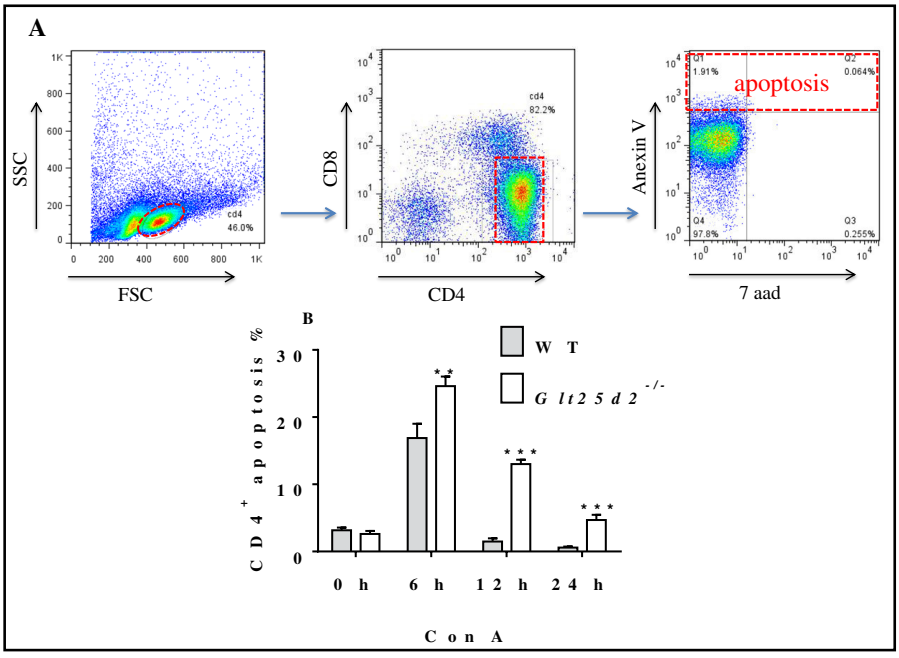

Fig. 8. Apoptosis analysis of primary CD4⁺ T cells. A, Gating method used to identify CD4⁺T cells and their apoptosis subsets. B, Apoptosis of CD4⁺ T cells was analyzed before and after concanavalin A (Con A) challenge for 0, 6, 12, or 24 h. The column diagram shows the frequency difference in apoptosis between wild-type (WT) and Glt25d2$^{-/-}$ CD4⁺ T cells before and after Con A challenge for 0, 6, 12, or 24 h (*P<0.01; ***P<0.0001).

CD25⁻CD69⁺ subset in splenocytes was significantly increased after Con A challenge for 12 h (7.41% ± 0.96% *vs* 4.00% ± 2.02%, $P = 0.001$) compared with those in WT mice (Fig. 6). The other notable result was that the subset frequency of *Glt25d2*$^{-/-}$ CD4⁺ T cells was significantly different from that in WT CD4⁺ T cells at baseline (before Con A challenge).

Glt25d2 knockout increased frequency of the CD25⁺CD69⁻ subset but decreased frequency of the CD25⁻CD69⁺ subset in primary CD4⁺ T cells

To further define the functional role of GLT25D2 in Con A–induced hepatitis, the CD4⁺ T cells were isolated from splenocytes and challenged with Con A (5 μg/mL) for 0, 6, 12, or 24 h. The frequency of the CD25⁺CD69⁻ subset was significantly increased in *Glt25d2*$^{-/-}$ CD4⁺ T cells after Con A challenge for 0 h (8.94% ± 0.37% *vs* 4.75% ± 0.38%, $P < 0.0001$), 6 h (8.85% ± 0.56% *vs* 3.49% ± 0.36%, $P < 0.0001$), 12 h (9.97% ± 0.19% *vs* 5.05% ± 1.13%, $P < 0.0001$), or 24 h (16.78% ± 0.41% *vs* 11.14% ± 0.47%, $P < 0.0001$) compared with those in WT CD4⁺ T cells. However, the frequency of the CD25⁻CD69⁺ subset was markedly decreased in *Glt25d2*$^{-/-}$ CD4⁺ T cells after Con A challenge for 6 h (11.04% ± 0.69% *vs* 28.77% ± 1.56%, $P < 0.0001$), 12 h (6.27% ± 0.27% *vs* 11.05% ± 0.96%, $P < 0.0001$), or 24 h (4.42% ± 0.20% *vs* 6.50% ± 0.44%, $P < 0.0001$) compared with those in WT CD4⁺ T cells (Fig. 7).

Activation-induced apoptosis increased in Glt25d2$^{-/-}$ *CD4⁺ T cells*

Since the proper function of T lymphocytes is correlated with glycosylation status, we also determined whether the apoptosis of CD4⁺ T cells changed after *Glt25d2* knockout. We observed the apoptosis rate of primary CD4⁺ T cells from WT and *Glt25d2*$^{-/-}$ mice after challenge with Con A (5 μg/mL) for 0, 6, 12, or 24 h. Subsequently, the cells were stained with fluorescently tagged annexin V antibody and 7-AAD. As expected, the activation-induced apoptosis was significantly increased in CD4⁺ T cells from *Glt25d2*$^{-/-}$ mice after Con A challenge for 6 h (24.62% ± 4.00% *vs* 16.88% ± 5.65%, $P = 0.0085$), 12 h (13.02% ± 1.60% *vs* 1.49% ± 1.24%, $P < 0.0001$), and 24 h (4.70% ± 1.86% *vs* 0.59% ± 0.42%, $P < 0.0001$) compared with those in CD4⁺ T cells from WT mice (Fig. 8).

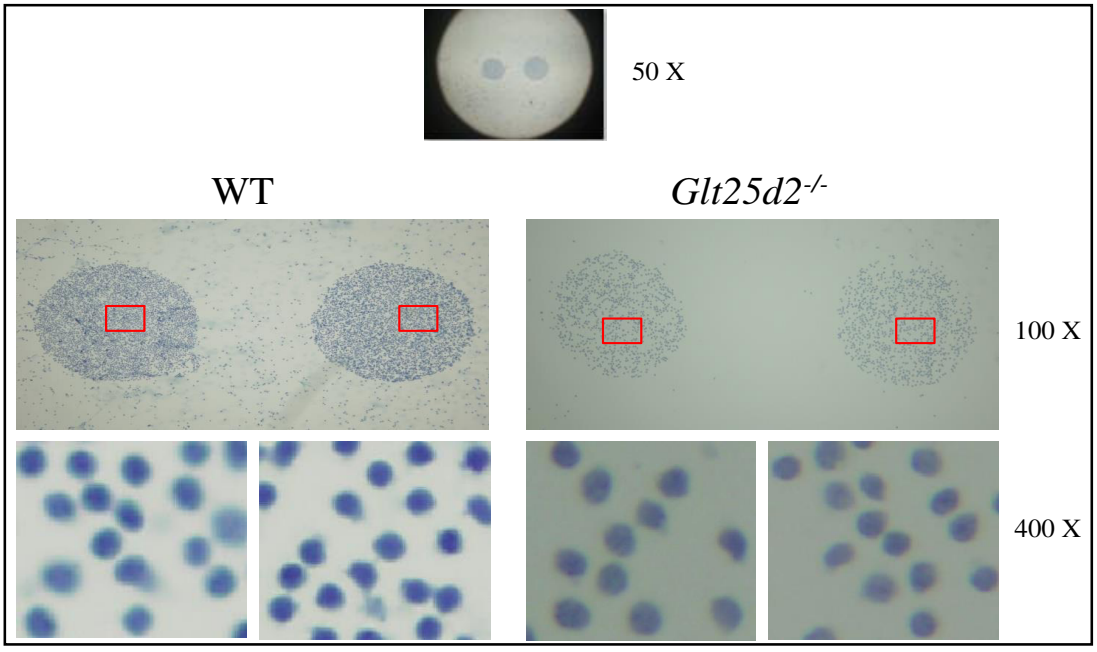

Fig. 9. Lectin array analysis of CD4+ T cells. To test the surface glycan repertoires between wild-type (WT) and Glt25d2$^{-/-}$ CD4+ T cells, the lectin array was used to determine the lectin-binding signatures. After isolation by magnetic beads labeled with CD4 monoclonal antibody and challenge with concanavalin A for 6, 12, or 24 h, CD4+ T cells were harvested and then incubated on a lectin array at 37°C for 1 h. Hematoxylin and eosin staining was performed after three phosphate buffered saline washes. The lectin-binding signature was observed by microscopy. ACL staining of WT CD4+ T cells and WFL staining of Glt25d2$^{-/-}$ CD4+ T cells are shown here.

Lectin-binding signature for CD4+ T cells during Con A challenge

The lectin-binding signature was determined to characterize the differences in cell surface glycan repertoires between WT and *Glt25d2*$^{-/-}$ CD4+ T cells (Fig. 9). *Glt25d2* knockout significantly increased the binding activities of several lectins. The *Wisteria floribunda* lectin (WFL)-, hippeastrum hybrid lectin (HHL)-, wheat germ agglutinin, *Galanthus nivalis* lectin (GNL)-, and *Narcissus pseudonarcissus* leptin (NPL)-binding activities were only observed in *Glt25d2*$^{-/-}$ CD4+ T cells; in contrast, the MPL- and *Erythrina cristagalli* lectin (ECA)-binding activities were found only in WT CD4+ T cells. *Glt25d2* knockout seemed to have no significant effect on the binding activities of soybean agglutinin lectin, *Maackia amurensis* leucoagglutinin 1 (MAL1), *Amaranthus caudatus* lectin (ACL), or jackfruit lectin of CD4+ T cells under normal conditions (Table 2).

Table 2. Lectin-binding signature of wild type (WT) and Colgalt2$^{-/-}$ CD4+T cells

	Control		Con A 6 h		Con A 12 h		Con A 24 h	
	WT	Colgalt2$^{-/-}$	WT	Colgalt2$^{-/-}$	WT	Colgalt2$^{-/-}$	WT	Colgalt2$^{-/-}$
MPL	+	-	-	+	-	-	-	-
ECA	+	-	-	-	-	-	+	-
WFA	-	+	-	-	-	-	-	-
HHL	-	+	+	+	+	+	+	+
WGA	-	+	-	-	-	-	+	-
GNL	-	+	+	+	+	+	+	+
NPL	-	+	-	+	-	-	-	+
SBA	+	+	+	+	+	-	+	+
MAL-I	+	+	-	-	-	-	-	-
ACL	+	+	+	-	+	-	+	-
Jacalin	+	+	-	+	+	+	+	-

Since glycoform reconstruction occurs during T lymphocyte activation, we also determined the surface glycoform variation of CD4+ T cells for Con A–induced activation at 6, 12, and 24 h. Table 2 shows that *Glt25d2* knockout increased binding of NPL to CD4+ T cells, whereas ACL-binding activity was lost. The binding activities of several lectins, namely, MAL1, WFA, MPL, and ECA, were lost during Con A stimulation, whereas those of HHL and GNL were increased irrespective of CD4+ T cell genotype (WT *vs Glt25d2*$^{-/-}$) (Table 2).

Discussion

Collagen structure is critical to $CD4^+$ T cell regulation [37], but the effect of collagen glycosylation on $CD4^+$ T cell regulation remains unknown (14, 17). Using our *Glt25d2*$^{-/-}$ mouse model, we found that *Glt25d2* knockout regulated the frequency of $CD4^+$ T cell subsets involved in Con A–induced hepatitis.

Glycosylation of the collagen protein was discovered nearly 60 years ago (10), and only recently were three gene products considered candidate glycosyltransferases, namely, lysyl hydroxylase 3 (12), GLT25D1, and GLT25D2 [13, 38, 39]. In one of these studies, GLT25D2 was shown to mediate Glcα1, 2Galβ1 glycosylation of hydroxylysine in collagen proteins (13). Using our *Glt25d2*$^{-/-}$ mouse model, we found that *Glt25d2* knockout directly aggravated liver injury and increased the inflammatory response after Con A challenge. Based on the present data and recent results, IL-4, IL-6, IL-1β, and IL-9 may complicate this process [40, 41]. Some chemokines, such as MIP-2, eotaxin, and GROα, were also significantly increased in *Glt25d2*$^{-/-}$ mice after Con A challenge compared with those in WT mice. The above results suggested that *Glt25d2* knockout may result in an abnormal chemotactic response to inflammatory cells.

Based on a recent report, GLT25D2 is a glycotransferase that mediates Glcα1, 2Galβ1 glycosylation of hydroxylysine in collagen and is involved in collagenous fibrils assembling into collagen fibers [13]. Since many proteins contain collagen domains and are involved in T cell regulation, as recent reports stated [42], we considered that GLT25D2 could mediate Glcα1, 2Galβ1 glycosylation of other collagen-like proteins in primary $CD4^+$ T cells *in vitro* and play a role in $CD4^+$ T cell regulatory processes such as proliferation and apoptosis. $CD4^+CD25^-CD69^+$ T cells are a novel subset of regulatory T cells that suppress T cell proliferation [43] and play a role in anti-graft-versus-host disease in humans [44]. We recently also found that the $CD25^-CD69^+$ subset of $CD4^+$ T cells is also involved in Con A–induced hepatitis [45]. To put our data in a wider context, the relative decrease in the $CD25^-CD69^+$ subset suggested that the $CD4^+$ regulatory T cells may be partly suppressed in *Glt25d2*$^{-/-}$ mice.

Our present results demonstrate for the first time that glycosylation mediated by GLT25D2 regulates the subset frequency of $CD4^+$ T cells. However, the molecular mechanisms of how surface glycoform changes influence the subset differentiation of $CD4^+$ T cells requires elucidation. As shown in a previous report [35] and confirmed here, altering cell surface glycan repertoires leads to different subset differentiation of $CD4^+$ T cells. Different from hyposialylation (*Cmah*$^{-/-}$ mice) leading to T lymphocyte proliferation and activation [46], inhibiting Glcα1, 2Galβ1 glycosylation (*Glt25d2*$^{-/-}$ mice) resulted in a different subset of $CD4^+$ T cells. As described above, many cell surface proteins may also be targets of GLT25D2 since they contain a collagen domain, such as mannan-binding lectin, which directly regulates T cell proliferation [47]. Therefore, we speculated that the differences in the lectin-binding signature resulted from the *Glt25d2* knockout *in vitro*. *Glt25d2* knockout increased the binding activity of NPL to $CD4^+$ T cells, whereas ACL-binding activity was lost. This result suggests that other receptor substrates of GLT25D2 may exist in $CD4^+$ T cells since NPL and ACL mainly recognize the terminal mannose Galβ1, 3GalNAc of cell surface glycans.

In contrast to findings of a previous study in human tissue [21], the present data show that GLT25D2 is broadly expressed in the spleen, thymus, and other tissues of mice. This expression difference may be due to species differences. The major limitation of the present study is that all the data are based on primary $CD4^+$ T cells *in vitro*. *Glt25d2* knockout may lead to more complicated subset differentiation of $CD4^+$ T cells *in vivo*. Based on a recent report, GLT25D1 may partly play a compensatory role in collagen glycosylation after *Glt25d2* knockout [48]. The exact role of Glcα1, 2Galβ1 glycosylation in collagen secretion and $CD4^+$ T differentiation remains to be clarified.

Since the collagen glycosylation mediated by GLT25D2 (and GLT25D1) is initiated in the ER, we speculated that $CD4^+$ T cell regulation by GLT25D2 may be via two major pathways: (i)

directly modifying collagen and influencing ECM structure; and (ii) modifying some proteins containing collagen domains that are located on the surface of $CD4^+$ T cells, such as C-type lectins [49], playing a very important indirect role in $CD4^+$ T cell regulation.

The present results suggest that collagen glycosylation mediated by GLT25D2 may be involved in regulating proliferation of $CD4^+$ T cell subsets and correlated with the pathogenesis of immune hepatitis. Collagen Glcα1, 2Galβ1 glycosylation mediated by GLT25D2 may be a new target of drug development for immune regulation and protection against liver injury.

Abbreviations

Ab (antibody); WT (wild type); MPL (maclura pomifera lectin); ECA (erythrina cristagalli lectin); WFA (wisteria floribunda lectin); HHL (hippeastrum Hybrid lectin); WGA (wheat germ agglutinin); GNL (galanthus nivalis lectin); NPL (narcissus pseudonarcissus lectin); SBA (glycine Max lectin); MAL-I (maackia amurensis lectin I); ACL (axinella corrugata).

Acknowledgements

This work was supported by grants from the National Natural Science Foundation of China (NNSFC 30872243 and NNSFC 81271901); Natural Science Foundation of Beijing (7152073) (to Prof. H.Wei); and NNSFC 20672144 (to Prof Q. He).

Disclosure Statement

The authors declare no competing financial interests.

References

1 Khokha R, Murthy A, Weiss A: Metalloproteinases and their natural inhibitors in inflammation and immunity. Nat Rev Immunol 2013;13:649-665.
2 Hallmann R, Zhang X, Di Russo J, Li L, Song J, Hannocks MJ, Sorokin L: The regulation of immune cell trafficking by the extracellular matrix. Curr Opin Cell Biol 2015;36:54-61.
3 Brown FD, Turley SJ: Fibroblastic reticular cells: organization and regulation of the T lymphocyte life cycle. J Immunol 2015;194:1389-1394.
4 Frey H, Schroeder N, Manon-Jensen T, Iozzo RV, Schaefer L: Biological interplay between proteoglycans and their innate immune receptors in inflammation. Febs J 2013;280:2165-2179.
5 Nastase MV, Young MF, Schaefer L: Biglycan: a multivalent proteoglycan providing structure and signals. The journal of histochemistry and cytochemistry :J Histochem Cytochem 2012;60:963-975.
6 Nickmann M, Saemisch M, Wilbert-Lampen U, Nickel T, Edelman ER, Methe H: Cell matrix contact modifies endothelial major histocompatibility complex class II expression in high-glucose environment. Am J Physiol Heart Circ Physiol 2013;305:H1592-1599.
7 Jobling R, D'Souza R, Baker N, Lara-Corrales I, Mendoza-Londono R, Dupuis L, Savarirayan R, Ala-Kokko L, Kannu P: The collagenopathies: review of clinical phenotypes and molecular correlations. Curr Rheumatol Rep 2014;16:394.
8 Mienaltowski MJ, Birk DE: Structure, physiology, and biochemistry of collagens. Adv Exp Med Biol 2014;802:5-29.
9 Ishikawa Y, Bachinger HP: A molecular ensemble in the rER for procollagen maturation. Biochim Biophys Acta 2013;1833:2479-2491.
10 Rosenbloom J, Blumenkrantz N, Prockop DJ: Sequential hydroxylation of lysine and glycosylation of hydroxylysine during the biosynthesis of collagen in isolated cartilage. Biochem Biophys Res Commun 1968;31:792-797.

11 Spiro RG, Lucas F, Rudall KM: Glycosylation of hydroxylysine in collagens. Nat New biol 1971;231:54-55.
12 Wang C, Luosujarvi H, Heikkinen J, Risteli M, Uitto L, Myllyla R: The third activity for lysyl hydroxylase 3: galactosylation of hydroxylysyl residues in collagens *in vitro*. Matrix Biol 2002;21:559-566.
13 Schegg B, Hülsmeier AJ, Rutschmann C, Maag C, Hennet T: Core glycosylation of collagen is initiated by two beta(1-O)galactosyltransferases. Mol Cell Biol 2009;29:943.
14 Gorgun G, Anderson KC: Intrinsic modulation of lymphocyte function by stromal cell network: advance in therapeutic targeting of cancer. Immunotherapy 2011;3:1253-1264.
15 Rommerswinkel N, Niggemann B, Keil S, Zänker K, Dittmar T: Analysis of cell migration within a three-dimensional collagen matrix. J Vis Exp 2014:e51963.
16 Popovic ZV, Wang S, Papatriantafyllou M, Kaya Z, Porubsky S, Meisner M, Bonrouhi M, Burgdorf S, Young MF, Schaefer L, Grone HJ: The proteoglycan biglycan enhances antigen-specific T cell activation potentially via MyD88 and TRIF pathways and triggers autoimmune perimyocarditis. J Immunol 2011;187:6217-6226.
17 Fulop T, Khalil A, Larbi A: The role of elastin peptides in modulating the immune response in aging and age-related diseases. Patho Biol 2012;60:28-33.
18 Savino W, Smaniotto S, Mendes-da-Cruz DA, Dardenne M: Growth hormone modulates migration of thymocytes and peripheral T cells. Ann N Y Acad Sci 2012;1261:49-54.
19 Warren KJ, Iwami D, Harris DG, Bromberg JS, Burrell BE: Laminins affect T cell trafficking and allograft fate. J Clin Invest 2014;124:2204-2218.
20 Ciechomska M, Wilson CL, Floudas A, Hui W, Rowan AD, van Eden W, Robinson JH, Knight AM: Antigen-specific B lymphocytes acquire proteoglycan aggrecan from cartilage extracellular matrix resulting in antigen presentation and CD4+ T-cell activation. Immunology 2014;141:70-78.
21 Kim CH: Crawling of effector T cells on extracellular matrix: role of integrins in interstitial migration in inflamed tissues. Cell Mol Immunol 2014;11:1-4.
22 Overstreet MG, Gaylo A, Angermann BR, Hughson A, Hyun YM, Lambert K, Acharya M, Billroth-Maclurg AC, Rosenberg AF, Topham DJ, Yagita H, Kim M, Lacy-Hulbert A, Meier-Schellersheim M, Fowell DJ: Inflammation-induced interstitial migration of effector CD4(+) T cells is dependent on integrin alphaV. Na Immunol 2013;14:949-958.
23 Loubaki L, Hadj-Salem I, Fakhfakh R, Jacques E, Plante S, Boisvert M, Aoudjit F, Chakir J: Co-culture of human bronchial fibroblasts and CD4+ T cells increases Th17 cytokine signature. PloS One 2013;8:e81983.
24 Pokidysheva E, Zientek KD, Ishikawa Y, Mizuno K, Vranka JA, Montgomery NT, Keene DR, Kawaguchi T, Okuyama K, Bachinger HP: Posttranslational modifications in type I collagen from different tissues extracted from wild type and prolyl 3-hydroxylase 1 null mice. J Biol Chem 2013;288:24742-24752.
25 Terajima M, Perdivara I, Sricholpech M, Deguchi Y, Pleshko N, Tomer KB, Yamauchi M: Glycosylation and cross-linking in bone type I collagen. J Biol Chem 2014;289:22636-22647.
26 Wei H, Li H, Ren H, Hao X, Wang Z, Liu R, Huang Y, Chen L, Wang H, Li B: Preparation and genotyping identification of GLT25D2 knockout mice. Chin J Exp Clin Virol 2013; 27:492-4 (in Chinese).
27 Heymann F, Hamesch K, Weiskirchen R, Tacke F: The concanavalin A model of acute hepatitis in mice. Lab Anim 2015;49:12-20.
28 Volarevic V, Misirkic M, Vucicevic L, Paunovic V, Simovic Markovic B, Stojanovic M, Milovanovic M, Jakovljevic V, Micic D, Arsenijevic N, Trajkovic V, Lukic ML: Metformin aggravates immune-mediated liver injury in mice. Arch Toxicol 2015;89:437-450.
29 Moldenhauer LM, Diener KR, Thring DM, Brown MP, Hayball JD, Robertson SA: Cross-presentation of male seminal fluid antigens elicits T cell activation to initiate the female immune response to pregnancy. J Immunol 2009;182:8080-8093.
30 Piccirillo CA, Letterio JJ, Thornton AM, McHugh RS, Mamura M, Mizuhara H, Shevach EM: CD4(+)CD25(+) regulatory T cells can mediate suppressor function in the absence of transforming growth factor beta1 production and responsiveness. J Exp Med 2002;196:237-246.
31 Selvaraj RK: Avian CD4(+)CD25(+) regulatory T cells: properties and therapeutic applications. Dev Comp Immunol 2013;41:397-402.
32 Mani H, Kleiner DE: Liver biopsy findings in chronic hepatitis B. Hepatology 2009;49:S61-71.
33 Nichols WC, Seligsohn U, Zivelin A, Terry VH, Hertel CE, Wheatley MA, Moussalli MJ, Hauri HP, Ciavarella N, Kaufman RJ, Ginsburg D: Mutations in the ER-Golgi intermediate compartment protein ERGIC-53 cause combined deficiency of coagulation factors V and VIII. Cell 1998;93:61-70.

34 Hauri HP, Kappeler F, Andersson H, Appenzeller C: ERGIC-53 and traffic in the secretory pathway. J Cell Sci 2000;113:587-596.
35 Shi YQ, He Q, Zhao YJ, Wang EH, Wu GP: Lectin microarrays differentiate carcinoma cells from reactive mesothelial cells in pleural effusions. Cytotechnology 2013;65:355-362.
36 Hnatiuk S, Barry M, Zeng W, Liu L, Lucas A, Percy D, McFadden G: Role of the C-terminal RDEL motif of the myxoma virus M-T4 protein in terms of apoptosis regulation and viral pathogenesis. Virology 1999;263:290-306.
37 Estes JD, Haase AT, Schacker TW: The role of collagen deposition in depleting CD4+ T cells and limiting reconstitution in HIV-1 and SIV infections through damage to the secondary lymphoid organ niche. Semin Immunol 2008;20:181-186.
38 Spaan Willy JM, Simone P, Liefhebber Jolanda MP, Van LHC: The human collagen beta(1-O) galactosyltransferase, GLT25D1, is a soluble endoplasmic reticulum localized protein. BMC Cell Biol 2010;11:33.
39 Perrin-Tricaud C, Rutschmann C, Hennet T: Identification of domains and amino acids essential to the collagen galactosyltransferase activity of GLT25D1. PloS One 2011;6:e29390.
40 Luo Q, Zhu L, Ding J, Zhuang X, Xu L, Chen F: Protective effect of galangin in Concanavalin A-induced hepatitis in mice. Drug Des Devel Ther 2015;9:2983-2992.
41 Proctor WR, Chakraborty M, Fullerton AM, Korrapati MC, Ryan PM, Semple K, Morrison JC, Berkson JD, Chea LS, Yang Q, Li AP, Spolski R, West EE, Rochman Y, Leonard WJ, Bourdi M, Pohl LR: Thymic stromal lymphopoietin and interleukin-4 mediate the pathogenesis of halothane-induced liver injury in mice. Hepatology 2014;60:1741-1752.
42 Li SS, Forslow A, Sundqvist KG: Autocrine regulation of T cell motility by calreticulin-thrombospondin-1 interaction. J Immunol 2005;174:654-661.
43 Han Y, Guo Q, Zhang M, Chen Z, Cao X: CD69+ CD4+ CD25- T cells, a new subset of regulatory T cells, suppress T cell proliferation through membrane-bound TGF-beta 1. J Immunol 2009;182:111-120.
44 Lu S, Huang X, Liu K, Liu D, Xu L: High frequency of CD4+ CD25- CD69+ T cells is correlated with a low risk of acute graft-versus-host disease in allotransplants. Clin Transplant 2012;26:E158-167.
45 Yang Q, Wang J, Liu R, Wang Z, Li Y, Zhang Y, Hao X, Huang Y, Xie W, Wei H: Amelioration of concanavalin A-induced autoimmune hepatitis by magnesium isoglycyrrhizinate through inhibition of CD4(+)CD25(-) CD69(+) subset proliferation. Drug Des Devel Ther 2016;10:443-453.
46 Buchlis G, Odorizzi P, Soto PC, Pearce OM, Hui DJ, Jordan MS, Varki A, Wherry EJ, High KA: Enhanced T cell function in a mouse model of human glycosylation. J Immunology 2013;191:228-237.
47 Zhao N, Wu J, Xiong S, Zhang L, Lu X, Chen S, Wu Q, Wang H, Liu Y, Chen Z, Zuo D: Mannan-binding lectin, a serum collectin, suppresses T-cell proliferation via direct interaction with cell surface calreticulin and inhibition of proximal T-cell receptor signaling. FASEB J 2017;31:2405-2417.
48 Baumann S, Hennet T: Collagen Accumulation in Osteosarcoma Cells lacking GLT25D1 Collagen Galactosyltransferase. J Biol Chem 2016;291:18514-18524.
49 Nabatov AA, de Jong MA, de Witte L, Bulgheresi S, Geijtenbeek TB: C-type lectin Mermaid inhibits dendritic cell mediated HIV-1 transmission to CD4+ T cells. Virology 2008;378:323-328.
50 Kleiner DE, Brunt EM, Van Natta M, Behling C, Contos MJ, Cummings OW, Ferrell LD, Liu YC, Torbenson MS, Unalp-Arida A, Yeh M, McCullough AJ, Sanyal AJ, Nonalcoholic Steatohepatitis Clinical Research N: Design and validation of a histological scoring system for nonalcoholic fatty liver disease. Hepatology 2005;41:1313-1321.